Stone Stability under Stationary Nonuniform Flows

Steenstra, Remco; Hofland, Bas; Paarlberg, Andries; Smale, Alfons; Huthoff, Fredrik; Uijttewaal, Wim

DOI
10.1061/(ASCE)HY.1943-7900.0001202

Publication date
2016

Document Version
Accepted author manuscript

Published in
Journal of Hydraulic Engineering (Reston)

This is an Accepted Manuscript of an article published by ASCE in Journal of Hydraulic Engineering
Volume 142 Issue 12 - December 2016,
available online: http://resolver.tudelft.nl/uuid:10.1061/%28ASCE%29HY.1943-7900.0001202

STONE STABILITY UNDER STATIONARY NON-UNIFORM FLOWS

Remco Steenstra [1] [2] Bas Hofland [3] [4] Alfons Smale [5]
Andries Paarlberg [6] Fredrik Huthoff [7] Wim Uijttewaal [8]

ABSTRACT

A stability parameter for rock in bed protections under non-uniform stationary flow is derived. The influence of the mean flow velocity, turbulence and mean acceleration of the flow are included explicitly in the parameter. The relatively new notion of explicitly incorporating the mean acceleration of the flow significantly improves the description of stone stability. The new stability parameter can be used in the design of granular bed protections using a numerical model, for a large variety of flows. The coefficients in the stability parameter are determined by regarding measured low-mobility entrainment rate of rock as a function of the stability parameter. Measurements of flow characteristics and stone entrainment of four different previous studies and many configurations (uniform flow, expansion, contraction, sill) are used. These configurations have different relative contributions of mean flow, turbulence and stationary acceleration. The coefficients in the parameter are fit to all data to obtain a formulation that is applicable to many configurations with non-uniform flow.

Keywords: Stone stability, Riprap, Turbulence, Acceleration

INTRODUCTION

Hydraulic structures like groins, breakwaters, bridge piers or pipeline protections are often built on a subsoil of sand. The hydraulic loads on the bed are increased by the presence of these

[1] Former graduate student, Delft Univ. of Technology, Environmental Fluid Mechanics Section, Delft, The Netherlands.
[2] Presently consultant, flux.partners, Amsterdam, The Netherlands, r.steenstra@flux.partners.
[3] Delft Univ. of Technology, Delft, The Netherlands, b.hofland@tudelft.nl.
[4] Deltares, Coastal Structures and Waves Department, Delft, the Netherlands.
[5] Deltares, Coastal Structures and Waves Department, Delft, the Netherlands.
[6] HKV Consultants, Lelystad, the Netherlands.
[7] HKV Consultants, Lelystad, the Netherlands.
[8] Delft Univ. of Technology, Delft, The Netherlands.

structures which can be the cause of erosion. The erosion of sand endangers the stability and the functioning of these structures and therefore this needs to be prevented. A frequently used method to do this is the use of granular bed protections. The weight of the stones that are used in the bed protections has to be large enough to withstand the forces that are exerted on them by the flow in order to maintain its function as bed protection.

The dimensions of hydraulic structures are often quite large which subsequently can lead to large surface areas that need to be covered by bed protections. Because of this, accurate methods of predicting the stability or damage to granular bed protections are desired.

A number of methods exists that can be used to predict the damage to granular bed protections. Most of the methods use a stability parameter to describe the forces that act on the stone. The stability parameter is then related to a certain measure for the damage, so that the stability parameter can be used to calculate the bed stability. The forces in the stability parameter are load caused by the flow, but also forces caused by the weight and the position of the stones.

The existing stability parameters are often derived for a limited range of applications. Shields (1936) derived a stability parameter for uniform flow, based on the bed shear stress. Other parameters (Maynord et al. 1989, for example) use the (near-bed) velocity to characterize the hydraulic attack. Also stability parameters have been derived that focus on the explicit incorporation of turbulence (Escarameia 1995; Jongeling et al. 2006; Hofland 2005; Hoan 2008; Hoffmans 2010). Other stability parameters look at the effects of pressure gradients in the flow on stone stability (Dessens 2004; Huijsmans 2006). If the above stability parameters are used outside their range of application, then the scatter of the data points is large and the prediction of the damage is inaccurate. Because of the inaccuracy in these design methods, in practice scale models are used to help guide the design of bed protections.

The hydrodynamic attack is usually given in terms of flow velocity or shear stress. However, the acceleration (or pressure gradient) in the flow also leads to a direct body force on bed material (Hoefel and Elgar 2003, for example). As the acceleration also influences the turbulence characteristics of the flow, both aspects have to be taken into account. In this paper several measurements of rock stability under a variety of stationary and non-uniform flow types are discussed. These measurements, in which velocity, turbulence properties and pressure gradients are known in detail, are used to determine a parameter that describes the influence of these flow characteristics explicitly and thus allow for a wider range of application as compared to the existing stability calculation methods.

This paper first discusses a number of methods to assess the stability of granular bed protections from literature in section 2. Then, section 3 proposes a new stability parameter based on the shortcomings of the stability parameters from literature. Section 4 gives an overview of the available data sets after which section 5 uses this data to evaluate a number of stability parameters, including the newly proposed stability parameter. Finally, this paper is concluded by a discussion and the conclusions.

LITERATURE

A commonly used method to describe the stability of a granular bed protections is by linking the damage to the forces that act on the stones. Much of the knowledge on incipient motion of granular bed protections is based on research on low mobility transport in gravel bed rivers. Bed protections also differs from gravel beds in some ways, specifically the more uniform grading and more angular shape of rock in bed protections, and at certain locations the higher level of turbulence in flow. A number of definitions to describe the damage are available, like for example the threshold of motion or the entrainment rate. To describe the forces that act on a stone a stability parameter is used. This dimensionless stability parameter is the ratio between destabilizing and resisting forces that act on the stones. Destabilizing forces are for example flow forces or gravity forces on a sloping bed. Examples of resisting forces are gravity and the forces due to surrounding stones. A lot of stability parameters have been derived over time, all with other purposes or derived with different measurements. This section first discusses some of these stability parameters after which different definitions of damage are discussed.

Stability parameters for uniform flow

One of the most well-known stability parameters is the one proposed by Shields (1936). See also the reviews of Buffington (1999), and Dey and Papanicolaou (2008). Shields (1936) assumed that the stability of a stone on the bed is determined by the bed shear stress τ_b and the submerged weight of the stones:

$$\Psi_S = \frac{\tau_b}{(\rho_s - \rho_w)gd} = \frac{u_\tau^2}{\Delta gd} \tag{1}$$

With τ_b the bed shear stress, u_τ the friction velocity,Δ the relative stone density ($\Delta = (\rho_s - \rho_w)/\rho_s$), ρ_s the mass density of the stones [kg/m^3], ρ_w the mass density of water, g the gravitational acceleration and d the stone diameter [m]. A similar stability parameter was introduced by Izbash (1935). In this parameter the numerator represents the square of the (local) mean velocity instead of the shear velocity.

The Shields parameter is derived for uniform flow and is therefore strictly speaking not applicable to non-uniform flow. It is possible to include the effects of turbulence in the Shields parameter by using an influence factor, see e.g. Schiereck (2001). These influence factors are often empirical relations based on specific flow situations resulting in a wide range of influence factors, lacking general validity. For every new or unknown situation, a new relation for the influence factor has to be derived. Another drawback is that the Shields parameter cannot predict the initiation of motion at locations with zero mean velocity but large fluctuations, like in reattachment points behind a backward-facing step.

Influence of the bed slope

The slope of the bed influences the initiation of motion of the rocks. Based on the force balance on a particle, the change in critical shear stress can be incorporated in a stability parameter. For a longitudinal bed slope this factor reads (Chiew and Parker 1994):

$$K_\beta = \frac{\phi - \beta}{\sin(\phi)} \tag{2}$$

With ϕ the angle of repose of the rocks and β the angle of the longitudinal slope. This relation is also used for bed protections (Schiereck 2001) A more general equation for the influence of a both longitudinal and transversal slope is also derived (Dey 2003, for example). In the present study only longitudinal slopes were considered.

Stability parameters with explicit incorporation of turbulence

Jongeling et al. (2003) propose a method that takes the turbulence into account more explicitly. The flow force (numerator) in this stability parameter is a combination of velocity and turbulence evaluated in the water layer above the location where the bed stability is regarded. The effect of turbulence is calculated as the square root of the turbulent kinetic energy k times an empirical turbulence magnification factor α. In this and the following stability parameters the stone diameter d is represented by d_{n50}, the nominal diameter (equivalent cube size) that is exceeded by 50% of the total mass of the stones.

Hofland (2005) proposed a similar stability parameter based on the assumption that large-scale velocity fluctuations can reach the bottom via an eddying motion. The large-scale velocity fluctuations at height z are assumed to be proportional to the square root of the turbulent kinetic energy $\sqrt{k}$. The fluctuations are part of a large rolling eddy so that the 'maximum velocity' at the bed can be determined using a length scale. The maximum of the local instantaneous velocity $(\overline{u} + \alpha\sqrt{k})$ at a certain height z is weighed with the relative mixing length L_m/z, since it is likely that the turbulent sources higher in the water column have less influence on the bed. Subsequently, the moving average with varying filter length L_m is taken of the weighted maximum velocity. Hofland (2005) found that using the Bahkmetev mixing length distribution l_m leads to the best results. The Hofland stability parameter is described in equation 3.

$$\Psi_{\mathrm{Lm}} = \frac{\max\left[\left\langle \overline{u} + \alpha\sqrt{k} \right\rangle_{l_m} \frac{\mathrm{l}_m}{z}\right]^2}{\Delta g d} \tag{3}$$

With $\overline{u}$ the mean velocity, k the turbulent kinetic energy, α an empirical turbulence magnification factor, $\langle ... \rangle_{l_m}$ the moving average with varying filter length l_m, l_m the Bahkmetev mixing length ($\kappa z\sqrt{1 - z/h}$), h the water depth and κ the Von Karman constant.

Comparable to the Hofland and Jongeling parameter, Hoan et al. (2011) proposed a stability parameter in which the turbulence closer to the bed has a larger influence on bed stability than the turbulence higher up in the water column. A weighting function is used to account for this. Hoffmans (2010) proposed a stability parameter with the depth-averaged turbulent kinetic energy added to account for the local turbulence. However, this stability parameter was not calibrated for non-uniform flows, so its use is limited to uniform flows. The Rock Manual (CUR, CIRIA, CETMEF 2007) describes the stability parameters of Pilarczyk (2001) and Escarameia (1995). To take into account the turbulence, influence factors for the stone diameter of up to 2 and higher are used in these stability parameters. These factors are case specific and difficult to estimate. Also, in the Rock Manual it is shown that these two approaches are not consistent for higher turbulence levels.

Stability parameters with incorporation of the pressure gradient

Dessens (2004) and Tromp (2004) give a stability parameter that includes the pressure gradient. Depth-averaged velocities and accelerations are used in the stability parameter, which is given in equation 4. Note that the acceleration term includes an extra stone diameter. This is because the force due to acceleration is a body force that acts on the volume ($\propto d^3$), while the drag and lift forces act on an area ($\propto d^2$).

$$\Psi_{MS} = \frac{\frac{1}{2} C_{\mathrm{b}} \overline{u}_{da}^2 + C_{\mathrm{m}} d \overline{a}_{da}}{\Delta g d} \tag{4}$$

With $\overline{u}_{da}$ the mean depth-averaged velocity, $\overline{a}_{da}$ the mean depth-averaged acceleration, C_b the combined drag and lift coefficient and C_m the added mass coefficient.

Dessens (2004) studied stationary acceleration in a contraction while Tromp (2004) studied time-dependent acceleration in waves. Dessens (2004) found values for C_b of 0.10 to 0.14 and for C_m of 3.9 to 5.6.

Damage

There are a number of methods available in theory to assess the stability of granular bed protections. The most well-known are the threshold of motion and the stone transport concept. In the first concept it is assumed that there is a certain condition at which incipient motion occurs and that stones start to move when this condition is exceeded. A critical value of the stability parameter is derived from measurements and used in the design of bed protections. The most well-known method that uses this concept is the one of Shields (1936). Jongeling et al. (2003) also gives a method that uses the threshold of motion in the design of bed protections.

The condition at which the threshold of motion occurs is rather subjective, since movement of stones can be interpreted in different ways. To partly overcome this problem, Breusers and Schukking (1971) defined 7 transport stages that go from no movement at all to general transport of the grains. Because of the irregularities in natural stones, the exposure of the stones and the irregular deviations from the mean flow characteristics due to turbulence, one general threshold of motion for the entire bed does not exist. Another disadvantage of the threshold of motion method, is that there is no information about the behaviour of the bed when the critical stability parameter is exceeded. This makes this method not usable for the design of for example maintenance programs for bed protections.

Another way to describe the stability of granular bed protections is in terms of stone transport. Here, the flow forces acting on the stones (written as a stability parameter Ψ) are linked to the bed response (as a dimensionless transport indicator Φ). The main advantage of this method is that it describes the behaviour of the bed after it becomes unstable. The general form of this relation is $\Phi = f(\Psi)$.

The dimensionless transport parameter Φ should represent the damage to the bed properly. Two ways of defining the transport of particles are distinguished. First there is the (volume) entrainment rate, this is the number of pick-ups per unit time and area. Second, the bed load transport can be used. This is the number of particles that is transported through a cross-section per unit time. Paintal (1971) provided a formula for low-mobility transport rates, also for dimensionless shear stresses under the 'critical' value of $\Psi = 0.05$.

Hofland (2005) states that because of the dependence of the bed load transport on upstream hydraulics (the stones passing a certain cross-section is a function of all the entrained stones upstream) the bed load transport is a non-local parameter. The entrainment rate, however, is completely dependent on local hydrodynamic parameters. The stability parameter Ψ also is a local parameter (solely depending on local flow characteristics). Hence here the entrainment rate is used to define and quantify the stability of the bed. The time dependence should be included in the entrainment rate, because due to turbulent fluctuations a stone moves sporadically and thus more stones are entrained during a longer period of time. The (volume) entrainment rate is described by equation 5.

$$E = \frac{nd^3}{AT} \tag{5}$$

In which E is entrainment rate, n the number of stones picked up, d the stone diameter, A the surface area and T the duration.

To describe the relation between the dimensionless transport parameter Φ and the stability parameter Ψ, often a power-law is used. The relation found by Hofland (2005) by using data from Jongeling et al. (2003) and De Gunst (1999) is shown in 1. The assumption was made that the initiation of motion is best described by a stability parameter where the correlation between a stability parameter Ψ and the dimensionless entrainment rate Φ_E is largest. This method is also applied presently. For a large variety of flow types the coefficients in the stability parameter are chosen such that the maximum correlation between Ψ and Φ_E is found.

PROPOSED STABILITY PARAMETER

In this paper, a new stability parameter is proposed that combines the effects caused by turbulence and the effects caused by the pressure gradient in stationary accelerating flows. The Hofland parameter is used for the influence of the velocity and turbulence and a pressure gradient is added to this parameter. The pressure gradient in accelerating flow can be approximated in different ways. Froehlich (1997) uses an expression based on buoyancy force that results from a water level gradient. Hofland (2005), Dessens (2004) and Huijsmans (2006) use an aproximation based on the Euler equation, which states that $a_x \approx -\frac{\partial p}{\partial x}$. Hence, building upon the expression in equation 3 the newly proposed stability parameter is given by equation 6, now including a pressure term.

$$\frac{\Psi^*_{new}}{C_{\mathrm{b}}} = \frac{\left(\max\left[\left\langle \overline{u} + \alpha\sqrt{k}\right\rangle_{Lm} \frac{L_m}{z}\right]^2\right) - C_{\mathrm{m}}/C_{\mathrm{b}}\frac{dp}{dx}d}{K_\beta \Delta g d} \tag{6}$$

In this equation, k is the turbulent kinetic energy, Lm the Bakmetev mixing length, z the height above the bed, $\overline{u}$ the mean (i.e. time-averaged) velocity, d the nominal stone diameter, d_{n50}, K_β the correction for the bed slope in the flow direction.

In the proposed stability parameter, the following three unknowns are present:

- C_{b} the bulk coefficient. Representing the relative importance of the force caused by velocity and turbulent velocity fluctuations. This parameter is a combination of the effects due to the drag, lift and shear forces.
- α an empirical turbulence magnification factor. This is the value of the turbulent velocity fluctuations represented by $\sqrt{k}$ relative to the mean velocity.
- C_{m} the added mass coefficient. This coefficient represents the force caused by the pressure gradient relative to the force due to the quasi steady forces.

The remainder of this article focuses on finding the unknowns in equation 6 and formulating an equation that predicts the dimensionless entrainment rate as function of the new dimensionless stability parameter. The relation that is used is a power law of the form $\Phi_E = a \cdot \Psi^b_{new}$. The unknowns are found by means of a correlation analysis. Further on, the unknowns C_m and C_b will be combined into one parameter C_m/C_b and the new stability parameter Ψ_{new} will be defined as Ψ^*_{new}/C_b. Measurements of flow characteristics (velocity, turbulent kinetic energy and pressure gradient) are coupled to the simultaneously measured entrainment rate. Before the correlation analysis is discussed, the next section first mentions the available data sets after which an evaluation is made on the usability of each data set.

DATA

This section discusses the data sets that are used in this paper. The data sets represent measurements of initiation of motion of coarse, angular bed material (hydraulically rough beds) under low transport conditions (entrainment rates corresponding to values of the Shields parameter well under the critical Shields factor for transport), and with detailed velocity measurements in the vertical above the location where the stone entrainment has been measured. As stone entrainment and the flow characteristics are measured at several locations for a single test setup, several data points, with varying mean flow, turbulence and acceleration characteristics are typically obtained for one flow configuration. This section first describes the data sets that have been used, after which an evaluation is made on the possibility to use the data sets in this research.

Data Used

The data that have been used are obtained at Deltares and the Delft University of Technology over the last decade. As not all data has been published yet in peer-reviewed journals, much of the data is re-analyzed presently. Table 1 summarizes the measurements that have been used in this paper.

Jongeling data

Jongeling et al. (2003) did measurements in a flume at Deltares with a length of 23 m, a width of 0.50 m and a height of 0.70 m for the following flow configurations, i.e.:

- Flow over a flat bed;
- Flow over a sill with a short crest;

- Flow over a sill with a long crest;

Bed material was used with a stone diameter of d_{n50} = 0.062 m, a grading width of d_{n85}/d_{n15} = 1.51, and a submerged relative density of Δ = 1.72. This was applied in a 4 cm thick layer on the flume floor. The bed was divided in coloured strips of 0.1 m length.

For the flat bed case, measurements were done over a 5.6 m long section, which was located behind a 13.6 long roughened initial section, to create uniform flow conditions. Water depths of about 0.25, 0.375, and 0.5 m were applied, with corresponding bulk mean velocities of respectively 0.7, 0.63 and 0.68 m/s. The short sill had an upstream slope and downstream slope of 1:8, a crest height of 0.12 m, and a crest width of 0.1 m. Measurements were made on the upstream slope (1 location), crest (2 locations), downstream slope (1 location), and downstream of the sill (6 locations). The long sill had an upstream slope of 1:8 and a downstream slope of 1:3, a crest height of 0.12 m, and a crest width of 2 m. Measurements were done on the crest (2 locations), and downstream of the sill (8 locations).

The velocity was measured by a combination of a 6 mW, forward scatter, Laser Doppler Velocimeter (LDV) and an Electro Magnetic velocity Sensor (EMS). The LDV measured the streamwise (u) and vertical (w) velocity components in a measurement volume with a 1 mm diameter and 10 mm transversal length, and the EMS measured the streamwise and transversal (v) velocity components in a roughly 1*1*1 cm measuring volume. The EMS measures a lower energy content as the velocity is averaged over a larger area, therefore k was determined by using the LDV results for the u and w components, and to correct v measured by the EMS by the ratio of the standard deviations of the longitudinal velocity components of LDV and EMS, $\sigma(u_{LDV})/\sigma(y_{EMS})$.

The discharge was measured by an electromagnetic device in the return flow, and the water levels were measured by a resistive type gauge.

The velocity was measured at different heights at a number of locations in the length of the flume, leading to a number of velocity profiles with their corresponding bed response. The stones at the bed that were located in a certain strip and had a certain colour. In this way, one could count how many stones moved and from what strips they originated. It should be mentioned that stones that move within their own strip are neglected when this method is used. Hofland (2005) suggested a correction factor for this, based on the probability distribution of the displacement length of the stones (see appendix D in Hofland (2005)). This correction is used on all the counted stones in this research.

Hoan data

Hoan et al. (2011) investigated the effect of increased turbulence on stone stability by analyzing measurements in an open-channel flow with symmetric, gradually expanding side walls in a laboratory flume. The flow width increased from 0.35 to 0.50 m. Three different expansions (3°, 5° and 7° for both side walls) were used to create different combinations of velocity and turbulence. No flow separation occurred at the side walls. Just as for the Jongeling data, flow velocities and the number of picked-up stones are measured.

The measurements were carried out at the Delft University of Technology in a flume with a width of 0.50 m and a height of 0.70 m. For the flow conditions a similar type of LDV was used. As only two velocity components (u and w) are available, the turbulence kinetic energy was approximated by assuming that $\sigma(v) = \sigma(u)/1.9$. The discharge was measured using an orifice plate in the inflow pipe.

Angular stones having a density of 2.700 kg/m^3, a nominal diameter of d_{n50} = 0.08 m, and d_{n85}/d_{n15} = 1.27 were placed at the horizontal flume bottom. The flow velocity during the experiments was too low to displace these natural stones. To examine stone stability, the top two layers of rock were replaced by uniformly coloured strips of artificial light stones at designated locations (0.1 m long by 0.2 m wide) on the flume axis before and along the expansion. These artificial stones were made of epoxy resin with densities in the range of 1,320 to 1,971 kg/m^3, mimicking shapes and sizes of natural stones. They had a nominal diameter of d_{n50} = 0.082 m and d_{n85} /d_{n15} = 1.11.

Dessens and Huijsmans data

Dessens (2004) and Huijsmans (2006) both investigated the effect of stone stability in accelerating flow by doing measurements in the same type of configuration. The same flume as in Hoan et al. (2011) was used, and a local contraction was created. Both used the same measurement instruments as Jongeling et al. (2003) and measured velocities, water levels and discharges. The stone transport was measured in the same way as Hoan et al. (2011). Different contraction angles were used, creating different combinations of velocities and accelerations.

Stones with a density of 2.680 kg/m^3 and two different stone sizes were used. One with a nominal diameter of d_{n50} = 0.02 m and the other with d_{n50} = 0.0082 m. The last 0.40 m of the contraction was covered with 0.10 m wide strips of coloured stones to measure the stone entrainment.

Discussion of the data sets

To be able to evaluate the parameters, the data sets have to contain the following information:

- velocity;
- turbulent kinetic energy;
- pressure gradient (or the stationary acceleration);
- entrainment rate.

The data sets of Hoan (2008), Dessens (2004) and Huijsmans (2006) can directly be used for the purposes of this article. In these data sets the pressure gradient was obtained from the measured free-surface slope. The data set of Jongeling et al. (2003), however, did not contain enough information for determining the pressure gradient dp/dx. Hence, a numerical model was created to determine the missing dp/dx at several measurements. The open source numerical solver OpenFOAM version 1.6-ext, see OpenFOAM Foundation (2012), has been used for this (Steenstra 2014).

Besides the additional numerical calculations for the Jongeling et al. (2003) data, the measured mean velocity and turbulence kinetic energy for all the different data sets have been calculated anew from the raw measurement data using the same processing script, in order to assure a uniform processing method.

ANALYSIS

The previous section discussed the data sets that are used in this research. These measurements will now be used to calculate a number of existing stability parameters and plot them against the measured dimensionless entrainment rate. After that, the unknowns in the proposed new stability parameter are determined by means of a correlation analysis. When these unknowns are determined, an analysis of the performance of the new stability parameter is made.

Existing stability parameters

Below, the measurements are used to calculate the Shields parameter, the Hofland parameter and the Dessens parameter. These parameters are subsequently plotted against the dimensionless entrainment rate derived from the measurements

Shields parameter

Figure 2 shows the Shields parameter plotted against the dimensionless entrainment rate. The shear stress velocity u_τ is calculated with equation 7 at the first data point located at a level z_1 above the bed.

$$u_\tau = \frac{\overline{u} \cdot \kappa}{\ln \frac{15 \cdot z_1}{(d_{n50})}} \quad (7)$$

The coefficient of determination R^2 (obtained through lineair regression) is 0.24 showing that much scatter is present. Especially the higher turbulence data points (like the long sill, short sill and the expansion) show a large deviation from the other data points.

For the flat bed only a few cases are included in the data sets. For these cases, the relationship between Ψ_S and Φ_E appears approximately linear (on the log-log scale). It can be seen that the data represent very low mobility with values of Ψ_S between 0.02 and 0.03, which is well below the initiation of motion criterion of Shields of 0.055. It is also still just below the first of 7 stages of increasing bed mobility: "displacement of grains, once in a while", which coincides with $\Psi_S \approx 0.03$ for coarse grains (Breusers and Schukking 1971), but within the range of low-mobility transport as measured by Paintal (1971).

Along the contraction the shear stress gets larger. According to the Shields parameter the bed shear stress is a destabilizing force and increasing bed shear stress causes increasing entrainment. Figure 2 clearly shows this behaviour in the accelerating flow (contraction) where for the same contraction, the entrainment rate increases with increasing Shields parameter. However, the data points in a contraction with a small side wall angle have, for equal entrainment, a larger Ψ_S than the contraction with a larger angle, indicating that the effect of acceleration itself (aside from the increased bed shear stress in accelerating flow) is not incorporated correctly in the Shields parameter.

For the expansion case with decelerating flow, very low correlation is seen between Ψ_S and Φ_E. Because of the decreased (shear) velocity in decelerating flow, Ψ_S decreases in decelerating flow and a decreasing entrainment rate would be expected. Figure 2 shows totally different behaviour. The entrainment rate in decelerating flow is rather uncorrelated to the Shields parameter. This can be attributed mainly to the absence of explicit incorporation of the turbulence in the Shields parameter.

The above shows that the bed shear stress is not a sufficient measure for predicting the damage to bed protections in non-uniform stationary flows.

Hofland parameter

The next existing stability parameter that is evaluated is the stability parameter Ψ_{Lm} from Hofland (2005).The parameter Ψ_{Lm} is defined in equation 3. Both Hofland and Booij (2006) and Hoan et al. (2011) determined the coefficients in this parameter. Hofland and Booij (2006) used the Jongeling et al. (2003) data set and found a value for the turbulence influence factor α of 6.0. Hoan et al. (2011) used his data of the expanding flows and found an α of 3.0. A relation between Ψ_{Lm} and Φ_E, using the values for the constants as derived by Hofland and Booij (2006), is plotted in figure 3. Using the constants as fitted by Hoan yields a similar graph.

The data points with relatively high turbulence and the data points of the flat bed simulation collapse well. The data points from the configurations with high accelerations show, for equal Ψ_{Lm}, much higher entrainment rates than those of the other cases, indicating that the entrainment rate is influenced by the pressure gradient in acceleration flows.

The Hofland stability parameter Ψ_{Lm} was designed to incorporate the effects of turbulence explicitly. Figure 3 shows that the parameter does this correctly, also for the newer data of Hoan et al. (2011). This confirms the findings of Hofland (2005), in which the behaviour of Ψ_{Lm} was analysed more extensive for the configurations of Jongeling et al. (2003). However, for the data points with a larger acceleration Ψ_{Lm} does not predict the entrainment rate accurately. Both Hofland (2005) and Hoan (2008) parameters will underestimate the entrainment in the contractions. This underestimation is attributed to the direct destabilizing effects of the pressure gradient on the stone stability.

Dessens parameter

Figure 4 shows the stability parameter proposed in Dessens (2004) (equation 4) plotted against the dimensionless entrainment rate. Remember that the effect of turbulence is not incorporated explicitely in this equation.

Figure 4 shows that using Ψ_{MS} leads to even larger scatter than using the Shields parameter Ψ_S. The value of R^2 is 0.028 for the entire set of used data in this article. This is almost a factor 10 smaller than the R^2 from the Shields parameter.

In contrast to figure 2, the contraction data points collapse well, which is not a coincidence because these are the data sets for which Ψ_{MS} was derived. The flat bed and part of the sill data points also collapse onto these data.

The measurement points that had high turbulence deviate a lot from the data points of the contraction. For these data points the entrainment rate is highly underestimated by the relation of Dessens (2004), which is derived for relatively small turbulence. The entrainment rate in the expansion shows almost no correlation with the stability parameter. The fact that these data points deviate from the trend for the accelerating flows can be explained by the fact that Dessens (2004) did not use an explicit formulation for the turbulence. Hence the influence of the turbulence was implicitly added to the drag/lift coefficient C_b. This ratio is apparently only applicable for the contraction and the flat bed cases.

The Dessens stability parameter Ψ_{MS} performs reasonably for situations with relatively small turbulence, such as in uniform or accelerating flows. As soon as there is increased turbulence, and there is no correction formula present for the change in relative turbulence, Ψ_{MS} does not predict the bed damage correctly at all.

Evaluation of the new stability parameter

The unknowns in equation 6 are determined by finding the combination of unknowns that lead to the highest correlation between the calculated stability parameter and the dimensionless entrainment rate. To minimize the number of unknowns it is chosen to combine the constants C_b and C_m into only one constant (see equation 8) and to define Ψ_{new} as Ψ^*_{new}/C_b.

$$C_{\text{m:b}} = \frac{C_{\text{m}}}{C_{\text{b}}} \tag{8}$$

Instead of the absolute value of C_b and C_m, now just the ratio between the two is calculated. For establishing a relation between Ψ_{new} and Φ_E, this is sufficient.

The steps that are taken in the correlation analysis are:

1. Set values for α, $C_{\text{m:b}}$
2. Calculate Ψ_{new} with equation 6
3. Find a and b in $\Phi_E = a\Psi^b$ through linear regression
4. Calculate the coefficient of determination $R^2 = 1 - \sum\left(\Phi_E - a\Psi^b_{\text{new}}\right)^2 / \sum\left(\Phi_E - \overline{\Phi_E}\right)^2$
5. Repeat steps 1 to 5 for a number of values of α and $C_{\text{m:b}}$

For α values of 0 to 7, with a step of 0.25 have been used. For $C_{\text{m:b}}$ values of 0 to 40, with a step of 1.0 have been used. Executing the method described above leads to the correlations shown in figure 5. The thick black line indicates the local maximum of R^2 for every $C_{m:b}$. The square dot indicates to absolute maximum with a R^2 of 0.80 with $\alpha = 3.75$ and $C_{m:b} = 23$. However, it should be mentioned that for values of $C_{\text{m:b}}$ larger than approximately 15.0 (and $\alpha = 3.0$), the value of R^2 remains approximately equal, with values around 0.79.

Equation 9 gives the final definition of the stability parameter Ψ_{new}. The first term in the nominator includes the forces that are caused by the velocity and the turbulent fluctuations that reach the bed. The second term accounts for the force caused by the pressure gradient due to acceleration.

$$\Psi_{new} \equiv \frac{\left(\max\left[\left\langle \overline{u} + \alpha\sqrt{k}\right\rangle_{Lm} \frac{Lm}{z}\right]^2\right) - C_{\text{m:b}} \frac{dp}{dx} d_{n50}}{K_\beta \cdot \Delta g d_{n50}} \tag{9}$$

The values for a and b in the power law $\Phi_E = a\Psi_{new}^b$ result from the regression analysis. Equation 6 gives the relation between the stability parameter and the bed response. The plot of this relation and the associated data points are given in figure 6.

The relation between the new stability parameter Ψ_{new} (for $\alpha = 6$ and $C_{m:b} = 23$) and the dimensionless entrainment rate Φ_E is given in equation 10 and plotted in figure 6 on log-log scale, and in figure 7 on a semi-log scale.

$$\Phi_E \equiv 3.95 \cdot 10^{-9} \Psi_{new}^{5.89} \qquad \text{for } 0.9 < \Psi_{new} < 4.3 \tag{10}$$

Table 2 gives some statistical quantities that followed from the regression analysis. These quantities can be used in for example probabilistic calculations. In the table the mean and standard deviation of the constants in $\Phi_E = a\Psi^b$ are given. Note that the a in this equation is not the acceleration.

From the analysis of the existing stability parameters it followed that the existing stability parameters were correlated to the dimensionless entrainment rate for the type of flow they were developed for, but that they did not perform for other types of stationary flows. The proposed new stability parameter Ψ_{new} from equation 10 includes, besides the influence of the mean flow velocity, both the influence of the (mean) pressure gradient as well as the explicitly described influence of the turbulence.

The correlation parameter for the relation between the Hofland stability parameter Ψ_{Lm} (with

$\alpha = 3.0$ and $C_{\text{m:b}} = 0$) and Φ_E, for the selected data sets, was 0.27. Using Ψ_{new} (with $\alpha = 3.75$ and $C_{\text{m:b}} = 23.0$ leads to a R^2 of 0.80. For the data sets used in this research, adding the effects of the pressure gradient in accelerating flow gives a considerable increase in correlation.

Table 3 gives the values for C_{b} and C_{m} from other sources. The value from ”theory” is based on the classic case of a sphere in a uniform flow. Here the drag coefficient is 0.4 (or somewhat higher if it is a blunt body) and the inertia coefficient is 2.0, such that $C_{\text{m:b}}$ = 5.0. This value can change with the shape of the rocks, but still seems rather small. This difference can be explained by the fact that the drag only acts on the top part of the rock (typically the rocks protrude 20% from the theoretical bed level), while the pressure gradient penetrates the bed to a much larger extent. This could make the relative influence of the inertia in the order of five times larger, which will yield values of $C_{\text{m:b}}$ in the same order as those found in the correlation analysis.

The value of $C_{\text{m:b}} = 23.0$ is roughly the average of the values found by Dessens (2004) and Tromp (2004). It also seems to be in the order of theoretical values. For now it is concluded that $C_{\text{m:b}} = 23.0$ is a plausible value for $C_{\text{m:b}}$ because it is within the rangeof previously found values and it predicts the effects of acceleration correctly in the stability parameter.

However, it should be mentioned that for values with a $C_{\text{m:b}}$ larger than 15.0, and their corresponding smaller α, the correlation remains approximately equal. Choosing a smaller $C_{\text{m:b}}$ and thus a smaller α can lead to less uncertainty in stability calculations since $\alpha\sqrt{k}$ is usually a large uncertainty if the output from a numerical model is used.

An example calculation from Steenstra (2014) shows that in the contraction (with most notable pressure gradient) the acceleration term increased the required rock size by approximately a factor 2 (so the weight by a factor 8). Contrary to this, in cases with decelerating flow the calculated rock size will be smaller when Ψ_{new} is used because the stabilizing effect of the adverse pressure gradient is included. This indicates that the acceleration has a significant influence on the required rock size in practice.

For design purposes a fixed value of Φ_E might be used as 'critical' value. For a uniform flow the Φ_E corresponding to a critical Shields factor of $\Psi \approx 0.03$, is $\Phi_E \approx 10^{-8}$ (Hofland 2005), see figure 2. According to figure 6 this corresponds to a value of the new parameter of $\Psi_{new,c} \approx 1.2$.

DISCUSSION

Some possible inaccuracies and limitations of the method are discussed next. A force generating mechanism that is not included in Ψ_{new} are the turbulent wall pressures. Turbulent wall pressures (i.e. fluctuating accelerations due to turbulence) can also entrain stones (Hofland 2005; Smart and Habersack 2007). This effect is not included explicitly in the stability parameter.

The entrainment rate is prone to scatter, as only several stones move per experiment, and the transport within a coloured strip has to be estimated. Moreover, the advective acceleration is used as approximation for the pressure gradient over the stone. This approximation can introduce errors.

Including both the effects of turbulence and the pressure gradient in the stability parameter greatly increases the range of application of the stability parameter compared to the already existing ones. However, the proposed stability parameter and its relation with the bed response is derived only for stationary acceleration. The effect of time-dependent acceleration (e.g. waves) should be investigated further before the proposed formulation can be used for that case. In wave action the value of the coefficient becomes a function of the wave period (acceleration period).

CONCLUSIONS

The stability of stones in bed protections is influenced by the quasi-steady forces, turbulent wall pressures and pressure gradients due to acceleration. Existing stability assessment methods do not incorporate all of these forces and are usually derived for only part of these forces. In this paper, a stability parameter is proposed that includes the influence of the mean flow velocity, turbulence and stationary acceleration in equation 9. Measurements of stone entrainment in a wide range of flow conditions and geometries are used to calibrate the constants in the proposed stability parameter. Missing data on pressure gradients were reconstructed by means of a computational model in the software package OpenFOAM.

The performance of several existing stability parameters was checked. It can be concluded that these parameters mainly can be used to obtain a relation between the stability parameter and the dimensionless entrainment rate (i.e. predict damage) for the flow type for which they were developed.

The proposed stability parameter Ψ_{new} shows the right behaviour for uniform, accelerating and decelerating flow, and thus has a wider range of application than the investigated existing stability parameters. The values of the derived α and $C_{\text{m:b}}$ are within the range of values that are derived in earlier research.A maximal correlation was obtained for α = 3.75 and $C_{\text{m:b}}$ = 23. The newly proposed stability parameter Ψ_{new} can be used in the design of bed protections to recognize the areas where larger (or smaller) stones are required, which can result in more efficient design of bed protections.

APPENDIX I. REFERENCES

Breusers, H. and Schukking, W. (1971). "Initiation of motion of bed material." *Tech. rept. S 151-1*, Deltares | Delft Hydraulics. (In Dutch).

Buffington, J. (1999). "The legend of A.F. Shields." *J. Hydraul. Eng*, 125(4), 376–387.

Chiew, Y. M. and Parker, G. (1994). "Incipient sediment motion on non-horizontal slopes." *J. Hydraul. Res.*, 32(5), 649 – 660.

CUR, CIRIA, CETMEF (2007). *The Rock Manual: The use of rock in hydraulic engineering*. London, 2nd edition.

De Gunst, M. (1999). "Stone stability in a turbulent flow behind a step." M.Sc. thesis. Delft University of Technology (In Dutch).

Dean, R. G. and Dalrymple, R. A. (1991.). *Water wave mechanics for engineers and scientists.* Singapore: World Scientific Publishing Co. Pte. Ltd.

Dessens, M. (2004). "The influence of flow acceleration on stone stability." M.Sc. thesis. Delft University of Technology, http://data.3tu.nl/repository/uuid:0ba04590-0c47-4e0c-80eb-979b2cc08e0c.

Dey, S. (2003). "Threshold of sediment motion on combined transverse and longitudinal sloping beds." *J. Hydraul. Res.*, 41(4), 405 – 415.

Dey, S. and Papanicolaou, A. (2008). "Sediment threshold under stream flow: A state-of-the-art review." *ASCE Journal of Civil Engineering*, 12(1), 45 – 60.

Escarameia, M. & May, R. W. P. (1995). "Stability of riprap and concrete blocks in highly turbulent flows.." *Proc. Instn Civ. Engrs Wat. Marit. & Energy*, (112), 227237.

Froehlich, D. C. (1997). "Riprap particle stability by moment analysis." *Proc. 27th congress of the IAHR*, San Francisco.

Hoan, N. T. (2008). "Stone stability under non-uniform flow." Ph.D. thesis. Delft Univerisity of Technology. http://data.3tu.nl/repository/uuid:cca1e773-4c36-4aa4-9ef7-38c86a0ed20e.

Hoan, N. T., Stive, M. J. F., Booij, R., and Verhagen, H. J. (2011). "Stone stability in non-uniform flow." *J. Hydraul. Eng*, 137(9).

Hoefel, F. and Elgar, S. (2003). "Wave-induced sediment transport and sandbar migration." *Science*, 299, 1885.

Hoffmans, G. (2010). "Stability of stones under uniform flow." *J. Hydraul. Eng*, 136(2), 129–136.

Hofland, B. (2005). "Rock & roll; turbulence-induced damage to granular bed protections". Ph.D. thesis. Delft University of Technology.

Hofland, B. and Booij, R. (2006). "Numerical modeling of damage to scour protections." *Third International Conference on Scour and Erosion,* Amsterdam, The Netherlands.

Huijsmans, M. A. (2006). "The influence of flow acceleration on the stability of stones." M.Sc. thesis. Delft University of Technology, http://data.3tu.nl/repository/uuid:6bd3d2b8-07e9-4742-a6fb-c78179c6a476.

Izbash, S. V. (1935). "Constructions of dams by dumping of stone in running water. Moscow, Leningrad.

Jongeling, T. H. G., Blom, A., Jagers, H. R. A., Stolker, C., and Verheij, H. J. (2003). "Design method granular protections." *Report No. Q2933 / Q3018*, WL | Delft Hydraulics. (december). In Dutch.

Jongeling, T. H. G., Jagers, H. R. A., and Stolker, C. (2006). "Design of granular bed protections using a RANS 3D-flow model." *Third International Conference on Scour and Erosion,* Amsterdam, The Netherlands.

Maynord, S. T., Ruff, J. F., and Abt, S. R. (1989). "Riprap design." *Journal of Hydraulic Engineering*, 115(7), 937–949.

OpenFOAM Foundation (2012). *OpenFOAM: The Open Source CFD Tool User Guide*, version 2.1.1 edition (May).

Paintal, A. S. (1971). "Concept of critical shear stress in loose boundary open channels." *Journal of Hydraulic Research*, 9, 91113.

Pilarczyk, K. W. (2001). "Unification of stability formulae for revetments." *XXIX IAHR congress* (September).

Schiereck, G. J. (2001). *Introduction to bed, bank and shore protection*. VSSD, Delft.

Shields, A. (1936). “Anwendung der aehnlichkeitsmechanik und der turbulenzforschung auf die geschiebebewegung.” *Mitteilungen der Preussischen Versuchsanstalt fuer Wasserbau und Schiffbau*. Berlin, Germany.

Smart, G. M. and Habersack, H. M. (2007). “Pressure fluctuations and gravel entraiment in rivers.” *J. Hydraul. Res.*, 45(5), 661 – 673.

Steenstra, R. S. (2014). “Incorporation of the effects of accelerating flow in the design of granular bed protections.” M.Sc. thesis. Delft University of Technology.

Tromp, M. (2004). “The influence that fluid accelerations have on the threshold of motion.” M.Sc. thesis. Delft University of Technology.

List of Tables

Source	Configuration Name	h [m]	Q [l/s]	No. of different Q and h	Measurement location	No. of measurement locations	No. of measurement points over depth	Bed slope i [-]	Width [m]	Sidewall angle [°]	dn50 [m]	Stone density ρs [kg/m3]	$\langle u\rangle_h$ [m/s]	Re [-]	ΦE [-]	dp/dx = rho*udu/dx [Pa/m]	<k>h [m2/s2]
Jongeling et al. [2003]	Flat bed	0,25	83,4	1	-	3	7	0.0	0,5	0.0	0.0062	2716	0.70	1,7E+05	2.8E-09	0.0	0.0044
		0,375	117,5	1	-	3	9	0.0	0,5	0.0	0.0062	2716	0.63	2,4E+05	5.0E-10	0.0	0.0031
		0,5	168,4	1	-	3	10	0.0	0,5	0.0	0.0062	2716	0.68	3,4E+05	7.2E-10	0.0	0.0028
	Long Sill: downstream slope 1:3	0,38	166,5	1	On sill	2	10	0.0	0,5	0.0	0.0062	2716	0.77	3,3E+05	4.9E-08	-13.4	0.0035
		0,5	166,5	1	Just behind sill	3	12	0.0	0,5	0.0	0.0062	2716	0.58	3,3E+05	4.8E-08	49.1	0.0126
		0,5	166,5	1	Further behind sill	5	12	0.0	0,5	0.0	0.0062	2716	0.68	3,3E+05	3.2E-08	8.3	0.0092
	Short Sill: downstream slope 1:8	0,45	189,4	1	Upward slope sill	1	10	0,125	0,5	0.0	0.0062	2716	0.88	3,8E+05	3.2E-08	255.9	0.0032
		0,38	189,4	1	Top sill	2	10	0.0	0,5	0.0	0.0062	2716	1.1	3,8E+05	1.8E-07	131.8	0.0026
		0,45	189,4	1	Downward slope sill	1	10	-0,125	0,5	0.0	0.0062	2716	0.82	3,8E+05	4.3E-08	-286.3	0.0067
		0,5	189,4	1	Behind sill	6	12	0.0	0,5	0.0	0.0062	2716	0.73	3,8E+05	3.6E-08	32.6	0.0088
Hoan [2008]	Expansion	0.12 - 0.19	22.0 - 35.5	12	In expansion	4	18 - 25	0.0	0.35 - 0.50	3.0	0.0082	1320 - 1971	0.40 - 0.47	5.0E04 - 10E04	2.3E-07 - 1.1E-06	-18.8	0.0035 - 0.0051
		0.12 - 0.19	22.0 - 35.5	12	In expansion	4	18 - 25	0.0	0.35 - 0.50	5.0	0.0082	1320 - 1971	0.36 - 0.44	4.3E4 - 10E04	1.7E-07 - 7.6E-07	-29,8	0.0034 - 0.0052
		0.12 - 0.19	22.0 - 35.5	12	In expansion	4	18 - 25	0.0	0.35 - 0.50	7.0	0.0082	1320 - 1971	0.38 - 0.47	5.0E4 - 10E04	1.8E-07 - 9.4E-07	-33.4	0.0036 - 0.0056
Huijsmans [2006]	Contraction 4.0°	0.246 - 0.285	30.0 - 60.0	3	In contraction	8	7	0.0	0.50 - 0.15	4.0	0.0082 and 0.02	2680	0.74 - 0.98	6.0E04 - 4.0E05	1.1E-06 - 8.1E-6	813.0	0.00047 - 0.00057
Dessens [2004]	Contraction 5.0°	0.260 - 0.438	30.0 - 60.0	3	In contraction	9	7	0.0	0.50 - 0.15	5.0	0.0082 and 0.02	2680	0.67 - 0.79	6.0E04 - 4.0E05	4.9E-07 - 8.6E-07	889.2	0.00046 - 0.00064
	Contraction 6.65°	0.257 - 0.434	30.0 - 60.0	3	In contraction	10	7	0.0	0.50 - 0.15	6.65	0.0082 and 0.02	2680	0.64 - 0.75	6.0E04 - 4.0E05	7.9E-07 - 1.1E-06	1017.7	0.00031 - 0.00045

TABLE 1. Summary of the measurements that have been used in this paper

	μ	σ
a	$3.95 \cdot 10^{-9}$	$6.3470 \cdot 10^{-10}$
b	5.89	0.2044

TABLE 2. Statistical quantities of the relation in equation 9

Research	**C_m/C_b**
Theory (e.g. (Dean and Dalrymple 1991))	$2.0/0.4 = 5$
(Dessens 2004)	39.2 - 39.6
(Tromp 2004)	4.85 - 9.375
This paper	23.0

TABLE 3. Values for C_m/C_b from other sources.

List of Figures

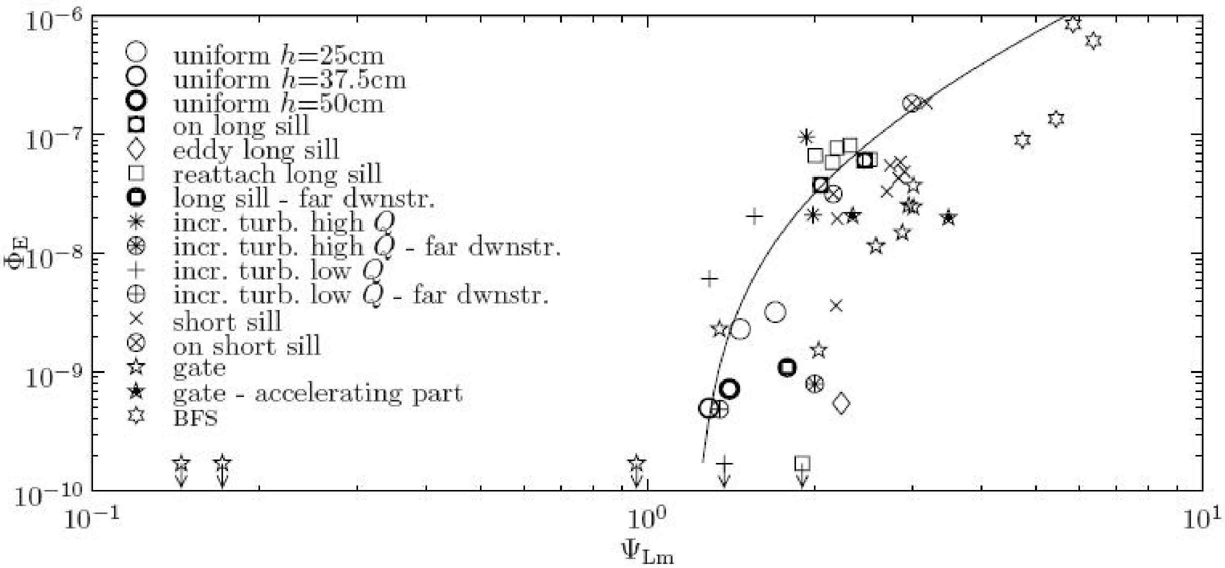

FIG. 1. The relation between Φ_E and $\Psi_{\mathbf{Lm}}$ as given by Hofland (2005)

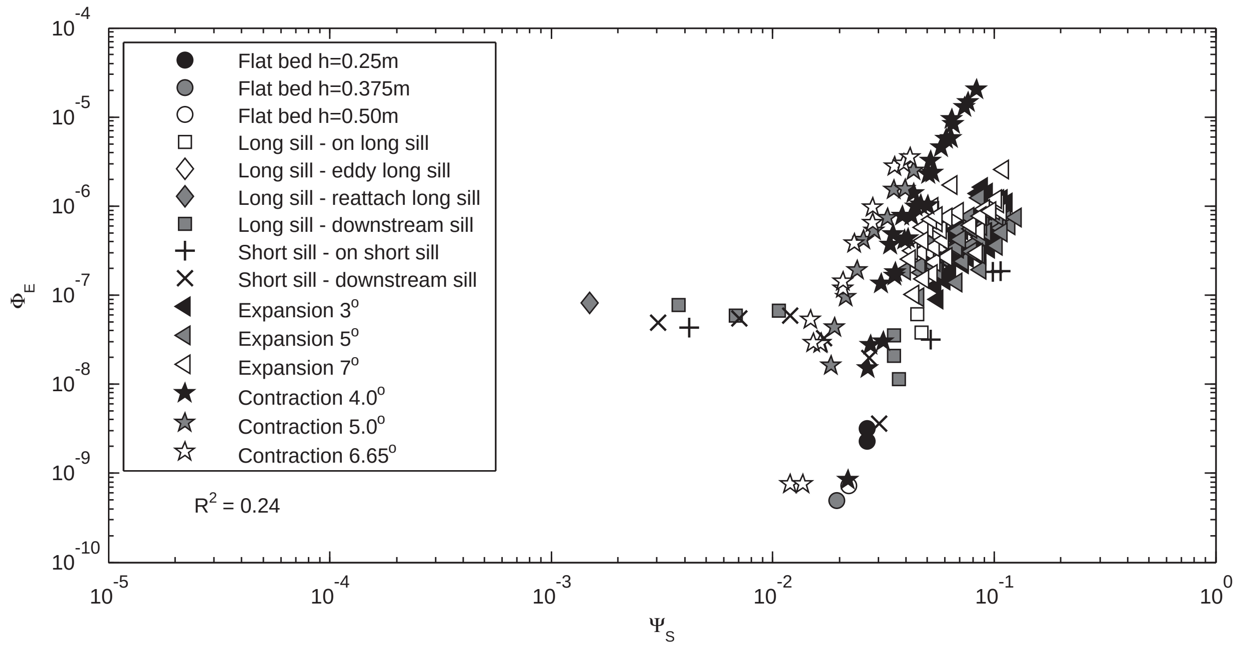

FIG. 2. The Shields parameter Ψ_S plotted against Φ_E for all the data sets

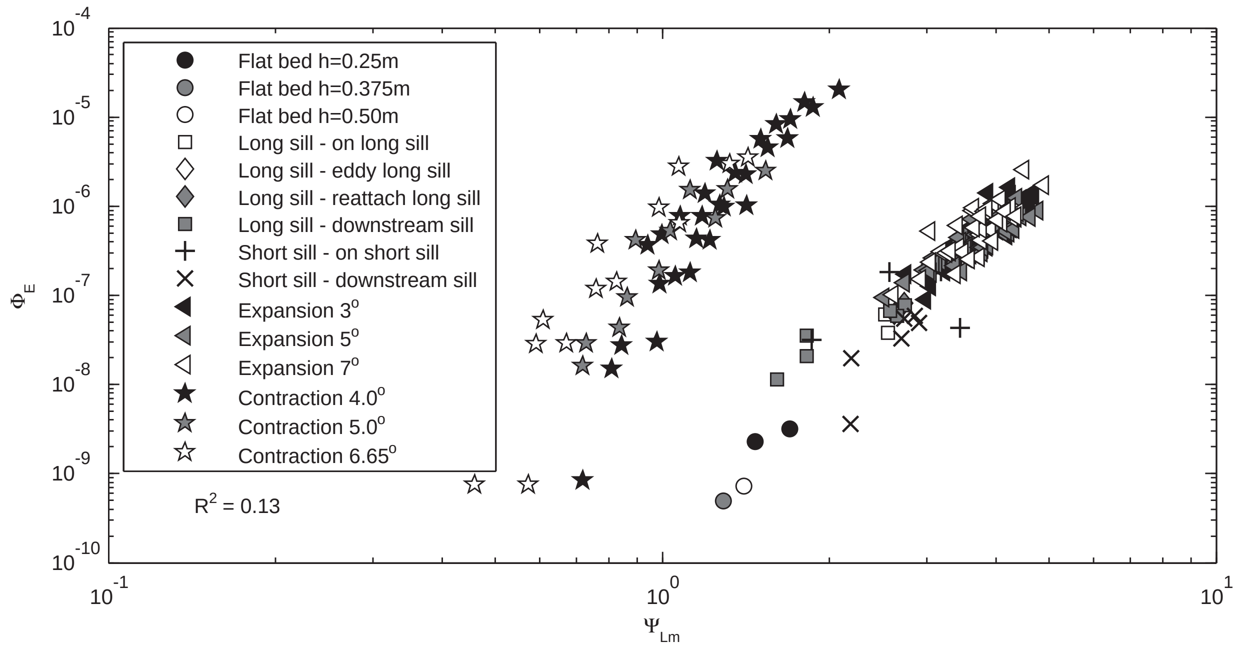

FIG. 3. $\Psi_{\mathbf{Lm}}$ **with** $\alpha = 6.0$ **plotted against** Φ_E

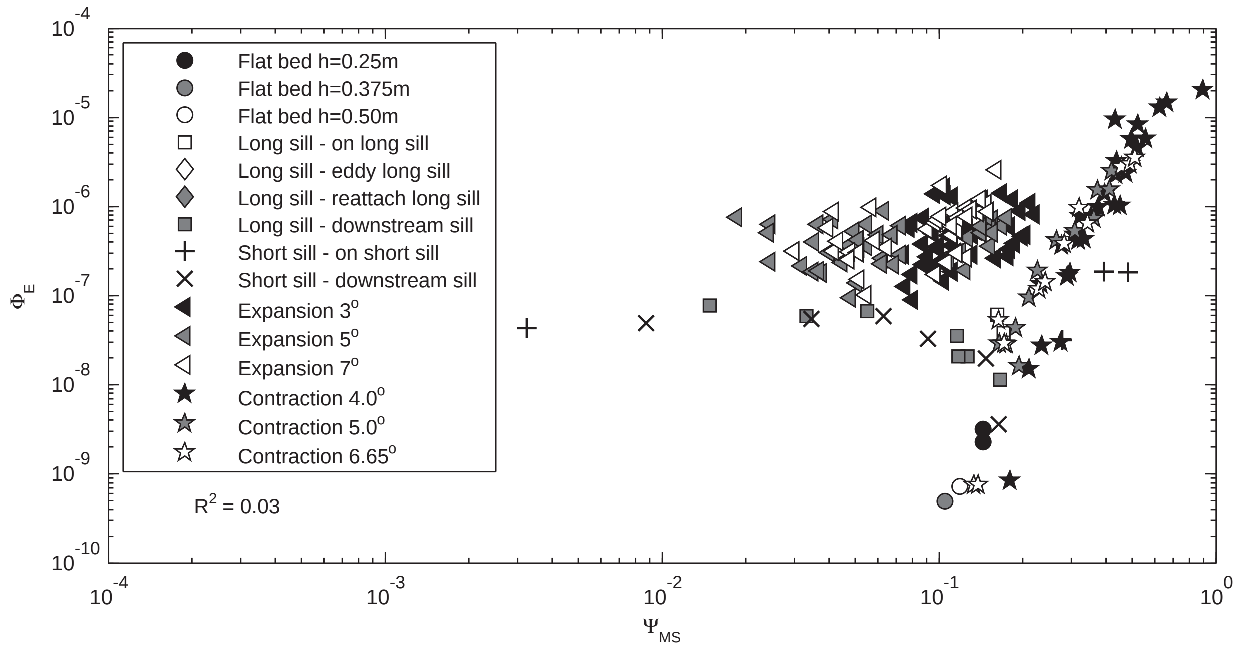

FIG. 4. The Dessens parameter $\Psi_{\mathbf{MS}}$ plotted against Φ_E for all the data sets

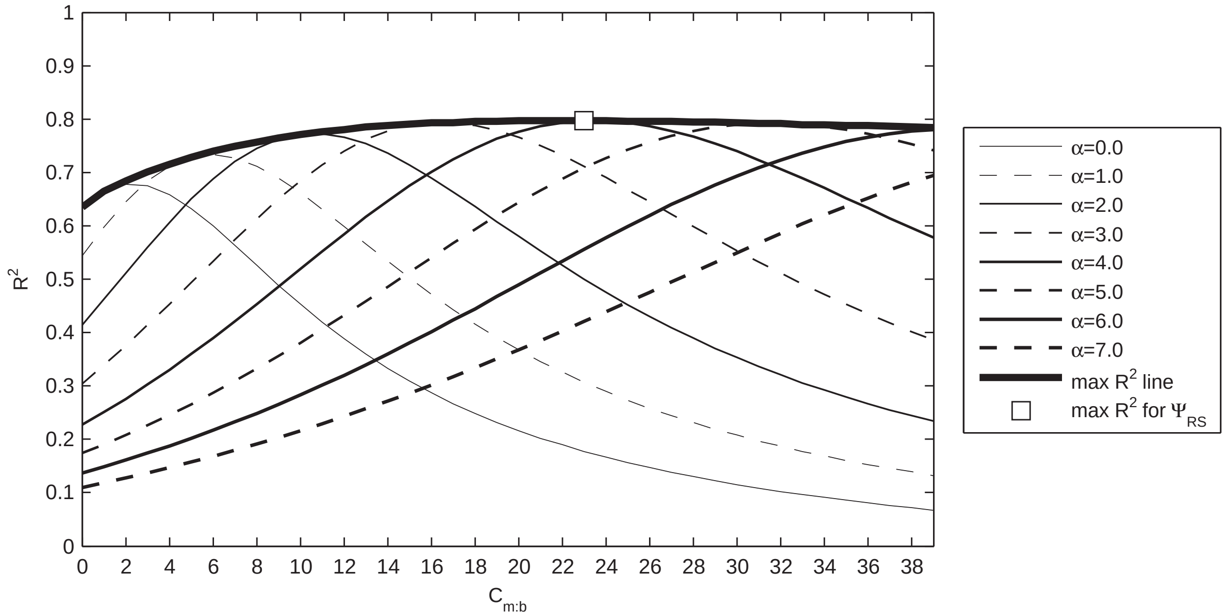

FIG. 5. R^2 **plotted against** $C_{\mathbf{m:b}}$**. The colored lines are the** R^2 **for different values of** α

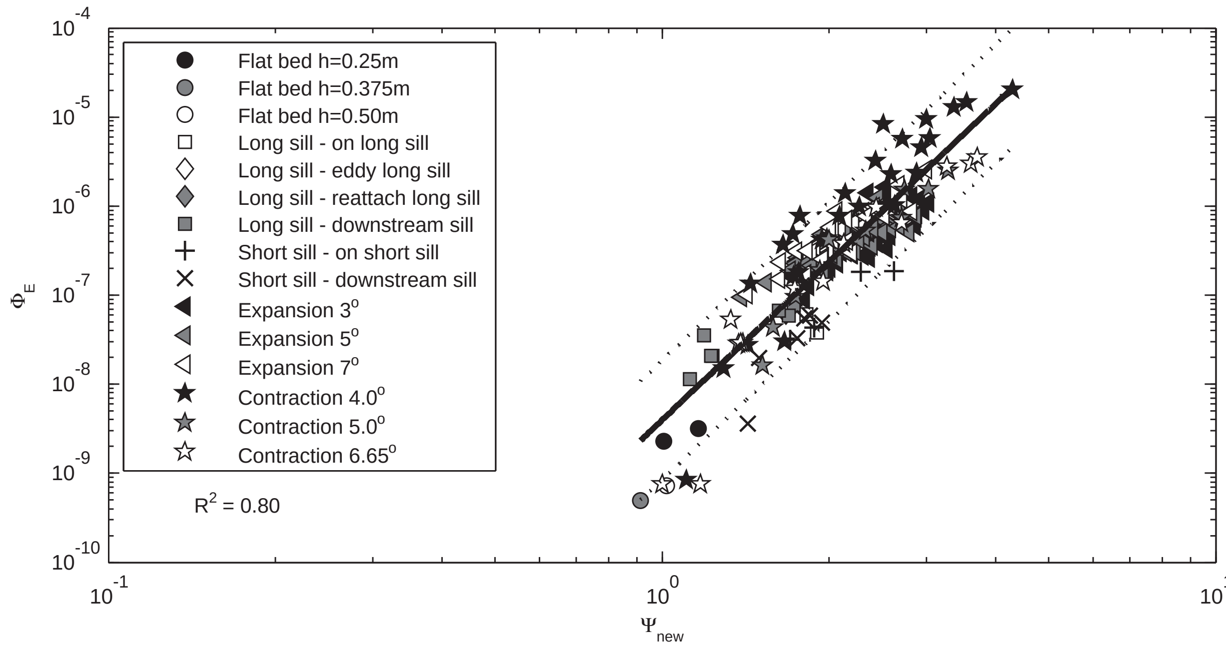

FIG. 6. Ψ_{new} **plotted against** Φ_E **for all the data sets on log-log scale**

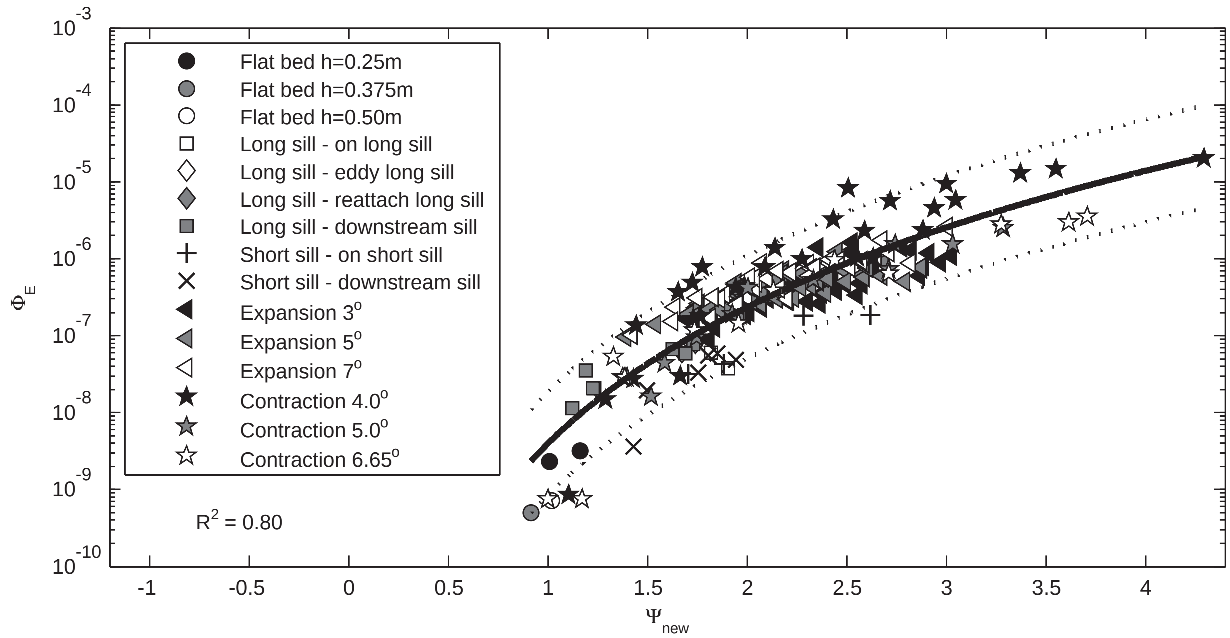

FIG. 7. Ψ_{new} **plotted against** Φ_E **for all the data sets on semi-log scale**